

Design and humanization of a murine scFv that blocks human platelet glycoprotein VI *in vitro*

Julien Muzard^{1,2}, Maxime Bouabdelli², Muhammad Zahid³, Véronique Ollivier², Jean Jacques Lacapère⁴, Martine Jandrot-Perrus² and Philippe Billiald^{1,3}

1 Muséum national d'Histoire naturelle, CNRS FRE 3206, CP39, Paris, France

2 Inserm U698, Hôpital Bichat, Université Paris 7, France

3 Université Paris-Sud 11, JE 2493, Faculté de Pharmacie, Châtenay-Malabry, France

4 Inserm U733, CRB3 Faculté Xavier Bichat, Université Paris 7, France

Keywords

antibody humanization; arterial thrombosis; collagen; platelet

Correspondence

P. Billiald, Museum national d'Histoire naturelle, CNRS FRE 3206, CP39, 12, rue Buffon, 75231 Paris cedex 05, France
Fax: +33 140 793 594

Tel: +33 140 793 155

E-mail: billiald@mnhn.fr

M. Jandrot-Perrus, Inserm U698, Hôpital Bichat, 46 rue Henri Huchard; University Paris 7, Paris, France

Fax: +33 140 258 602

Tel: +33 140 256 531

E-mail: martine.jandrot-perrus@inserm.fr

(Received 15 October 2007, accepted 3 June 2009)

doi:10.1111/j.1742-4658.2009.07129.x

Platelet adhesion and aggregation at the site of vascular injury is essential for hemostasis, but can also lead to arterial occlusion in thrombotic disorders. Glycoprotein (GP) VI is the major platelet membrane receptor that interacts directly with collagen, the most thrombogenic compound in the blood vessels. GPVI could therefore be a major therapeutic target. Fab fragments of the anti-GPVI murine monoclonal IgG 9O12 have previously been shown to completely block collagen-induced platelet aggregation, to inhibit the procoagulant activity of collagen-stimulated platelets, and to prevent thrombus formation under arterial flow conditions without significantly prolonging the bleeding time. Here, we engineered recombinant scFvs that preserve the functional properties of 9O12, and could constitute building blocks for designing new compounds with potentially therapeutic antithrombotic properties. First, the 9O12 variable domains were cloned, sequenced, and expressed as a recombinant murine scFv, which was fully characterized. This scFv preserved all the characteristics that make 9O12 Fab potentially useful for therapeutic applications, including its high affinity for GPVI, ability to inhibit platelet adhesion, and aggregation with collagen under arterial flow conditions. A humanized version of this scFv was also designed after complementarity-determining region grafting and structural refinements using homology-based modeling. The final product was produced in recombinant bacteria. It retained GPVI-binding specificity and high affinity, which are the main parameters usually impaired by humanization procedures. This is a simple, efficient and straightforward method that could also be used for humanizing other antibodies.

Introduction

Platelets play a crucial role in thrombus formation and limiting blood loss from sites of vascular injury. This is a complex process and entails the following series of steps: adhesion of platelets to the damaged vascular subendothelium, activation of the platelets, their

recruitment and, finally, aggregation. In some circumstances, such as disruption of the atherosclerotic plaques, platelet activation can lead to arterial occlusion and irreversible tissue damage. Acute coronary and cerebrovascular accidents usually result from this

Abbreviations

CDR, complementarity-determining region; FITC, fluorescein isothiocyanate; FR, framework region; GP, glycoprotein; PRP, platelet-rich plasma; SPR, surface plasmon resonance.

phenomenon, and they are currently the leading causes of death in the world. As a consequence, antiplatelet drugs constitute a major class of therapeutics intended to prevent and/or reverse platelet aggregation in arterial thrombosis [1]. Drugs that act on the platelet recruitment step have been used for a long time, and include inhibitors of cyclooxygenase (aspirin), phosphodiesterase inhibitors (dipyridamole) and, more recently, ADP receptor antagonists (clopidogrel). A chimeric antibody fragment (Fab) (abciximab) directed to glycoprotein (GP) IIb-GPIIIa that acts on the final step of the aggregation has also been approved for specific subsets of patients with acute coronary disease. However, all of the drugs currently utilized to counteract platelet function suffer from a lack of potency and/or specificity, and major risks of hemorrhage and thrombocytopenia are associated with their use [2]. There is therefore a continuing need for new and improved drugs that will inhibit platelet function in diseases characterized by thrombosis, and in particular for drugs with limited hemorrhagic effects, this point being crucial for safe antithrombotic therapy.

An attractive antithrombotic strategy would consist of targeting the initial interaction of platelets with the vessel wall rather than the later recruitment and aggregation phases. GPVI is the major receptor that interacts directly with collagen, which is the most thrombogenic compound in the vessel wall. GPVI mediates platelet aggregation and secretion of the secondary agonists responsible for thrombus growth. In addition, the release of growth factors and cytokines contributes to the recruitment of inflammatory cells and to the proliferation of smooth muscle cells, leading to stenosis [3,4]. Finally, GPVI expression is restricted to the platelet lineage [5]. There is also direct experimental and clinical evidence that platelets deficient in GPVI cannot be activated by collagen, and that a deficiency in GPVI expression does not produce major bleeding [6,7]. For all of these reasons, GPVI antagonists can be expected to be good candidates for preventing secondary thrombosis in an efficient and specific manner and also to be associated with a low risk of hemorrhage.

GPVI antagonists can be designed in several ways. One approach consists of generating soluble GPVI recombinant proteins or GPVI mimetics that will compete with platelets to bind to collagen. Encouraging results have been reported in a murine thrombosis model using the extracellular domain of murine GPVI produced in fusion with the human immunoglobulin Fc domain [8]. However, these results have not been confirmed, and the use of competitive ligands such as soluble recombinant GPVI may be associated with

considerable pharmacological and functional drawbacks [9]. A more effective way to block platelet GPVI–collagen interactions consists of directly targeting GPVI with molecules such as specific antibodies. Previous studies have shown that targeting murine GPVI with the rat monoclonal antibody JAQ1 abolishes collagen responses in circulating platelets, leading to the depletion of the receptor and to long-term anti-thrombotic protection in mice [10–12]. However, this antibody does not crossreact with human GPVI. Recombinant scFvs directed against human GPVI have also been reported over the last few years [13–15]. These antibody fragments have been isolated from combinatorial phage display libraries expressing human scFvs, and some of them specifically block GPVI binding to collagen under experimental conditions. However, they all exhibit low affinity for their target (K_D in the range of 10^{-7} M), making them unsuitable for therapeutic applications. Recently, monoclonal Fab fragments derived from four distinct murine hybridomas (OM 1–4) were found to inhibit the binding of GPVI to collagen, collagen-induced secretion and thromboxane A_2 formation *in vitro*, as well as *ex vivo* collagen-induced platelet aggregation after intravenous injection in cynomolgus monkeys [16,17]. Fab OM 4 also inhibited thrombus formation *in vivo* in rats without prolonging the bleeding time, thus confirming the therapeutic potential of antibody fragments directed to GPVI [18]. A human–mouse chimeric monoclonal antibody (cF1232) has also been reported to cause GPVI immunodepletion with a long-term *in vivo* antiplatelet effect in monkeys. However, such a process is not reversible and implies GPVI depletion on megakaryocytes, the consequence of which has not been addressed [19].

Another murine monoclonal antibody-derived Fab (9O12) specific for human GPVI has been developed and characterized by our group [20]. This high-affinity inhibitory monovalent Fab not only completely blocks collagen-induced platelet aggregation, but also inhibits the procoagulant activity of collagen-stimulated platelets, and prevents thrombus formation under both static and flow conditions. However, the immunogenicity of murine antibody fragments is a major obstacle to their clinical development, so it is necessary to reduce this immunogenicity by a humanization procedure.

Here, we report the cloning and sequencing of 9O12 variable domains, and the engineering and detailed evaluation of the derived scFv produced in recombinant bacteria. In view of its high potential, the murine scFv ($_m$ scFv 9O12) was then humanized. At this stage, the 9O12 complementarity-determining regions (CDRs) were grafted onto closely related human antibody

variable domains, and refinements were carried out after *in silico* modeling and inspection of the paratope. The cDNA encoding the humanized construct ($_m$ scFv 9O12) was chemically synthesized, cloned, and expressed in recombinant bacteria. We were able to purify this molecule and to test it on human platelets by flow cytometry analysis. The final product did not suffer loss of affinity and specificity, which are the parameters usually affected by humanization procedures.

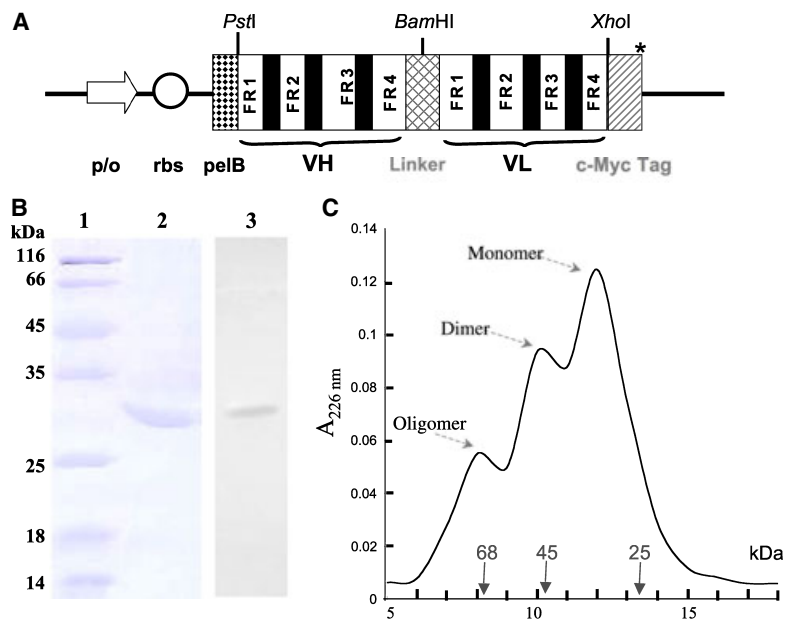
Results

Design, bacterial expression and purification of $_m$ scFv 9O12

cDNAs encoding the VH and VL domains of 9O12 were derived from hybridoma cell mRNA in an RT-PCR using consensus primers. Sequencing of the PCR product corresponding to the VH domain led to a single sequence, whereas the sequence of the PCR product corresponding to the VL domain was scrambled because of the amplification of the aberrant MOPC21-derived Vk gene. Digestion of the VL PCR product with *Bci*VI, and treatment as previously reported, made it possible to bypass the aberrant MOPC21-derived transcript, and to clone the 9O12 kappa light chain V-gene [21]. To ensure accuracy, VH and VL cDNAs were independently amplified from two distinct batches of mRNA. Sequencing confirmed that no mutation had occurred during the PCR reac-

tion. The 9O12 VH and VL cDNA sequences are now registered in the EMBL data bank (AM 887763 and AM 887764, respectively). The scFv-encoding gene derived from the variable regions of 9O12 [VH and VL linked together via a short linker (G_4S_3)] was then constructed, and inserted in frame with the pelB signal sequence, upstream of the c-Myc tag, into the pSW1 expression vector (pSW- $_m$ scFv 9O12). The construct is shown in Fig. 1A. Plasmid pSW- $_m$ scFv 9O12 was cloned into the TOPPI *Escherichia coli* strain, and the recombinant protein was produced and purified by affinity chromatography using GPVI-Sepharose gel. This procedure made it possible to recover fully functional scFv with a yield of $200 \mu\text{g}\cdot\text{L}^{-1}$ of culture. The preparation was homogeneous, as shown by SDS/PAGE under reducing conditions, western blot using the antibody against c-Myc, and MS analysis, which indicated an experimental relative molecular mass ($M + H^+$) of 28 402.3 Da, close to the theoretical molecular mass of 28 394.5 Da calculated from the amino acid sequence (Fig. 1B). The purified scFv was further analyzed by size exclusion chromatography (Fig. 1C). This revealed the presence of a main peak (62%) eluting at 12.5 mL with an apparent molecular mass of about 27 kDa, corresponding to the monomeric $_m$ scFv 9O12. Two other minor peaks were also observed: one eluted at 11 mL (25%), and the other at 8 mL (13%). These minor peaks could correspond to the dimeric and multimeric forms of $_m$ scFv, as previously reported for other scFvs [22]. After storage at 4 °C, the isolated dimeric and multimeric fractions

Fig. 1. Construction and structural characterization of $_m$ scFv 9O12. (A) Diagram of the expression vector pSW- $_m$ scFv9O12. The gene encoding $_m$ scFv 9O12 is cloned between the *Pst*I and *Xho*I sites in-frame with the pelB leader sequence and the c-Myc tag sequence followed by a stop codon (*). p/o, operon; rbs, ribosome-binding site; pelB, signal sequence. (B) Affinity-purified $_m$ scFv 9O12 analyzed after SDS/PAGE and staining with Coomassie brilliant blue (lane 2) or western blotting on nitrocellulose membrane and immunostaining using a monoclonal antibody against c-Myc (lane 3). Lane 1: molecular mass standards. (C) Size exclusion chromatography of affinity-purified $_m$ scFv 9O12 performed on a Superdex 75 HR 10/30 column calibrated versus standards of known molecular mass.



were subjected to another gel filtration step. This resulted in a two-peak elution profile, one peak corresponding to the dimer, and the other to the monomer. The proportion of monomer increased when the dimer fraction was left for 3 days before being reapplied, demonstrating the instability of dimers and higher-order oligomers (data not shown). Monomeric scFv remained stable after prolonged storage at 4 °C. Affinity-purified scFv 9O12, but not the irrelevant scFv 9C2, was able to bind to GPVI in a dose-dependent manner in a direct ELISA, and competed with 9O12 (data not shown).

Functional properties of m scFv 9O12

Analysis of the scFv–GPVI interaction in real time using surface plasmon resonance (SPR) technology allowed us to determine the kinetic parameters of m scFv 9O12 using the BIAcore 2000 system and BIA-EVALUATION version 3.1 software (BIAcore, Uppsala, Sweden) (Fig. 2A). This gave the following kinetic parameters: $k_{on} = 6.5 \times 10^4 \text{ M}^{-1}\cdot\text{s}^{-1}$, $k_{off} = 1.7 \times 10^{-4}\cdot\text{s}^{-1}$, and the dissociation constant $K_D = 2.6 \text{ nM}$. These parameters were similar to those calculated under the same conditions for the 9O12 proteolytic

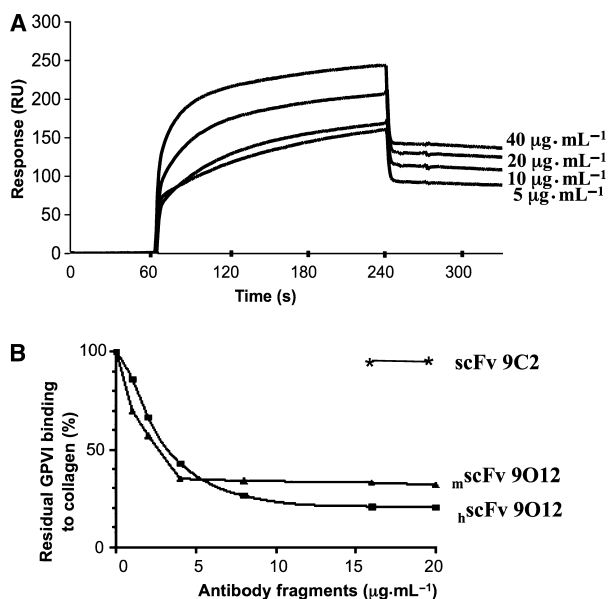


Fig. 2. Analysis of m scFv 9O12 binding to GPVI. (A) GPVI was immobilized on a CM5 sensor chip, and the binding of purified scFv 9O12 was analyzed by SPR after injection of increasing amounts. Nonspecific binding analyzed using scFv 9C2 has been subtracted. (B) Collagen was immobilized on a microtitration plate, and GPVI binding to collagen was investigated in the presence of increasing amounts of antibody: triangle, m scFv 9O12; square, 9O12 Fab; star, irrelevant scFv 9C2.

Fab fragment ($K_D = 2.3 \text{ nM}$) and parental IgG ($K_D = 4.0 \text{ nM}$). We investigated the ability of purified m scFv 9O12 to bind to immobilized GPVI after prolonged storage at 4 and 20 °C (for 3 days), and no significant decrease in antigen-binding ability was observed.

We also investigated whether the interaction of m scFv 9O12 with GPVI could inhibit the binding of GPVI to collagen immobilized on microtitration plates. GPVI preincubated with increasing amounts of antibody fragments was added to the wells. As shown in Fig. 2B, m scFv 9O12 inhibited GPVI ($20 \mu\text{g}\cdot\text{mL}^{-1}$) binding to collagen with an IC_{50} of approximately $1.17 \mu\text{g}\cdot\text{mL}^{-1}$, 80% inhibition being reached at a concentration of $5\text{--}10 \mu\text{g}\cdot\text{mL}^{-1}$ of m scFv 9O12. This inhibitory capacity was comparable to that observed for 9O12 Fab prepared after papain digestion of the parental IgG ($2.1 \mu\text{g}\cdot\text{mL}^{-1}$). Similar results were observed after incubation of GPVI (10 or $40 \mu\text{g}\cdot\text{mL}^{-1}$) with the antibody fragments. In contrast, the irrelevant scFv 9C2 had no effect on the binding of GPVI to collagen.

Effects induced by m scFv 9O12 binding to GPVI

The binding of m scFv 9O12 to native GPVI expressed at the platelet surface was further observed by flow cytometry, as indicated by the shift of the fluorescence peak to the right (Fig. 3A). Its ability to inhibit collagen-induced platelet aggregation was tested by light transmission aggregometry. The affinity-purified m scFv 9O12 ($25 \mu\text{g}\cdot\text{mL}^{-1}$) delayed the aggregation and reduced its extent from 65% to 25%, whereas the Fab was fully inhibitory (Fig. 3B). We further tested the monomeric form of m scFv 9O12 purified after size exclusion gel chromatography (Superdex 75 column) at the same concentration, and observed total inhibition of platelet aggregation, as observed with the Fab (not shown).

In addition, the effects of m scFv 9O12 on platelet adhesion and aggregation to collagen were investigated under arterial flow conditions, and compared with those of 9O12 Fab and an irrelevant scFv (Fig. 4). Once again, platelet aggregation induced by collagen was inhibited. In the presence of 9O12 fragments (scFv or Fab), only isolated platelets attached to the collagen fibers were observed, in agreement with previous results [20,23]. In contrast to control conditions, no large platelet aggregates were observed over a 5 min period.

As 9O12 Fab is known to inhibit thrombin generation at the surface of collagen-stimulated platelets, the effect of the purified m scFv 9O12 was tested using the thrombogram method (Fig. 5). m scFv 9O12 and 9O12

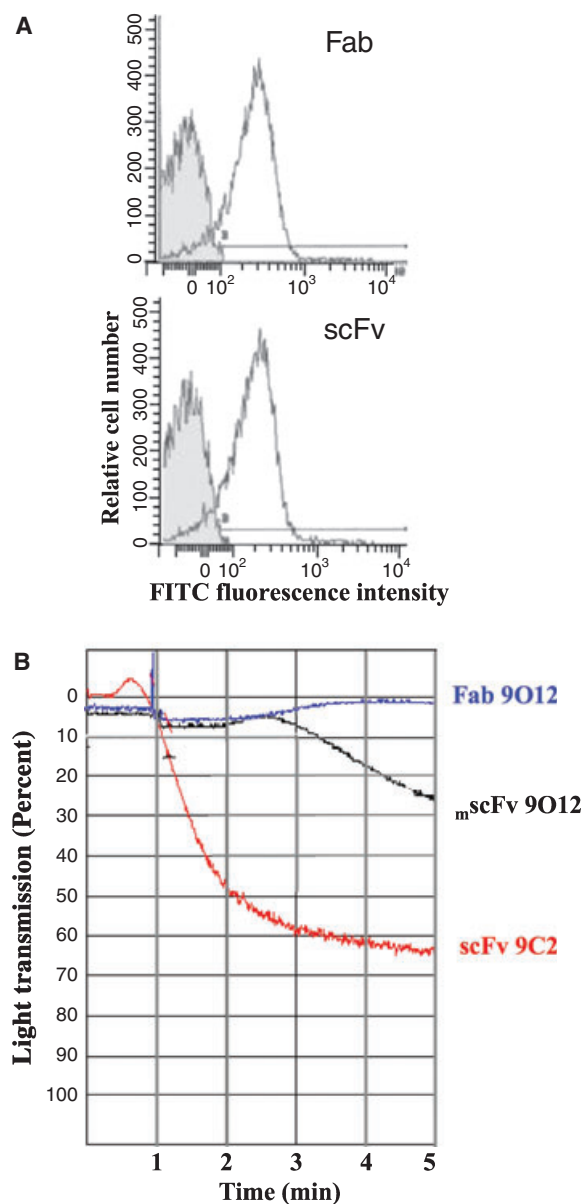


Fig. 3. Analysis of m scFv 9O12 binding to platelets. (A) Flow cytometry analysis: washed platelets were incubated for 30 min with antibody fragments ($40 \mu\text{g}\cdot\text{mL}^{-1}$): Fab (upper panel) and scFv (lower panel) revealed by a FITC-coupled anti-mouse Ig and by an FITC-coupled anti-c-Myc Ig, respectively. Dark line: 9O12 Ig fragments. Gray histogram: control 9C2 antibody fragments. (B) Effects of m scFv 9O12 on platelet aggregation induced by collagen. Washed human platelets were incubated with control scFv 9C2, 9O12 Fab or affinity-purified scFv 9O12 for 5 min at 37°C . Then, collagen was added. Aggregation was analyzed at 37°C while stirring, and the change in light transmission was recorded.

Fab reduced the thrombin peak to similar extents, and increased the lag preceding thrombin generation, indicating that m scFv 9O12 is as efficient as 9O12 Fab

in inhibiting collagen-induced platelet procoagulant activity.

Humanization of m scFv 9O12 and functional evaluation

Murine antibodies would trigger an immune reaction if injected into human beings, and so humanization is required before any clinical investigation can be undertaken. To do this, we first constructed a 3D structural model of m scFv 9O12 *in silico* after identifying the crystal structures with sequences very similar to the 9O12 variable domains. All of these sequences were of murine origin. The top four scoring structures of murine origin were used for modeling. For the VH gene, we used antibodies designated 1PLG, 1MNU, 1A5F and 1IGI in the Protein Data Bank, which have 66–78% sequence identity (79–85% similarity) with 9O12. For the VL gene, we used antibodies 1PLG, 1IGI, 1MNU, and 1AXT, which have 87–90% sequence identity (94–95% similarity). The 3D structures of all these sequences were solved with a resolution higher than 2.8 \AA . Twenty models were generated for each domain, using MODELER 3.0 software, and the best one was selected on the basis of the rmsd value (0.13 \AA for VH and 0.703 \AA for VL) and detailed inspection. The model is shown in Fig. 6A.

We then proceeded to the humanization of 9O12 variable domains. To do this, FASTA searches were performed to independently align VH and VL amino acid sequences against a repertoire of human antibody sequences registered in the Protein Data Bank. Among the human variable domains that matched 9O12, we first selected a VH domain and a VL domain from the same antibody molecule in order to preserve the inter-domain contacts that occur in a natural antibody. The human antibody 1VGE was selected because it had the best identity score with 9O12 when the entire variable domain sequences were spanned, and was found to exhibit 62% and 55% identity with the VH domain and VL domain, respectively. When calculated over framework region (FR) sequences alone, the identity was even slightly better, at 69.5% and 65.4%, respectively. In addition, the crystallographic structure of 1VGE was solved at high resolution (2 \AA and $R = 0.18$). We therefore decided to graft 9O12 CDRs onto the 1VGE template *in silico*. A gene encoding this construct was chemically synthesized, and inserted into pSWI exactly as had been done for m scFv 9O12. TOP-PI cells transformed with this vector were induced to express the recombinant protein. However, the recombinant protein was never detected in the periplasm of induced bacteria, and so some refinements of the

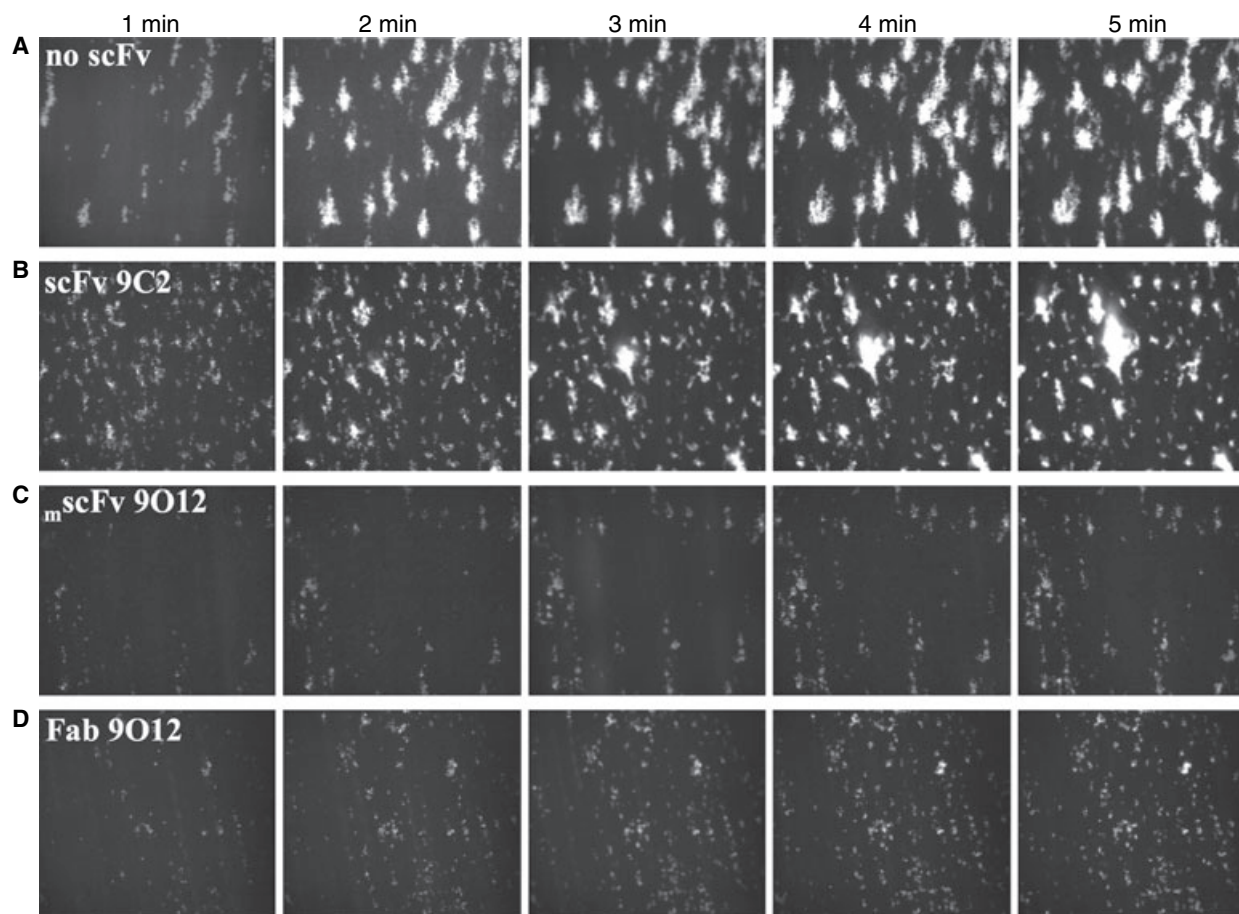


Fig. 4. Effect of m_{scFv} 9O12 on platelet aggregation induced by collagen under arterial flow conditions. Whole blood cells labeled with fluorochrome DIOC-6 were incubated with NaCl/P; (A) or antibody fragments (B–D), and then perfused onto collagen-coated coverslips in a flow chamber at 1500 s^{-1} . The formation of platelet aggregates bound to the collagen matrix was recorded with a fluorescence microscope at various time intervals. (B) Control scFv 9C2. (C) m_{scFv} 9O12. (D) 9O12 Fab.

construct were called for. First, we observed that 9O12 V-kappa CDR1 is five residues longer than that of the template (1VGE), and that 9O12 and 1VGE V-kappa FR1 and FR2 have low identity scores (48% and 73%, respectively) (Fig. 6C). Extra FASTA searches were then performed using 9O12 V-kappa FR1 and FR2. An excellent match was found with V-kappa FR1 and FR2 from human antibody 1X9Q (95.6% and 86.6% identity scores, respectively, and 100% similarity in both cases). In addition, V-kappa CDR1 of the selected antibody 1X9Q was similar in length to that of 9O12. We therefore decided to preserve the original 9O12 V-kappa FR1 and FR2 in the novel humanized scFv construction. Other refinements were carried out on the basis of close inspection of the model, and the final construct is shown in Fig. 6B. All of the humanized 9O12 frameworks exhibit 100% similarity with human frameworks, apart from the IGHV

and V-kappa FR3 (90.62% and 93.75%, respectively) (Table 1). The 11 N-terminal residues from the murine IGHV FR3 were preserved in the final construct, because they are clearly located close to the flat part of the pocket in which the antigen is expected, and so could interact with it. Nevertheless, IGHV FR3 exhibits 25/32 residue identity with 1VGE. Only three residues of this framework (Ala71, Lys73, and Arg76; Kabat numbering) had no similarity with 1VGE. The 9O12 V-kappa FR3 was substituted for its 1VGE counterpart, with the exception of two residues (L59P and D60S), essentially because Leu is not frequently encountered at this position, and Asp is an acidic residue.

The gene encoding the scFv in which humanized 9O12 variable domains are fused together via the short flexible linker $(G_4S)_3$ was synthesized and cloned into the pSW1 vector. The final humanized scFv 9O12

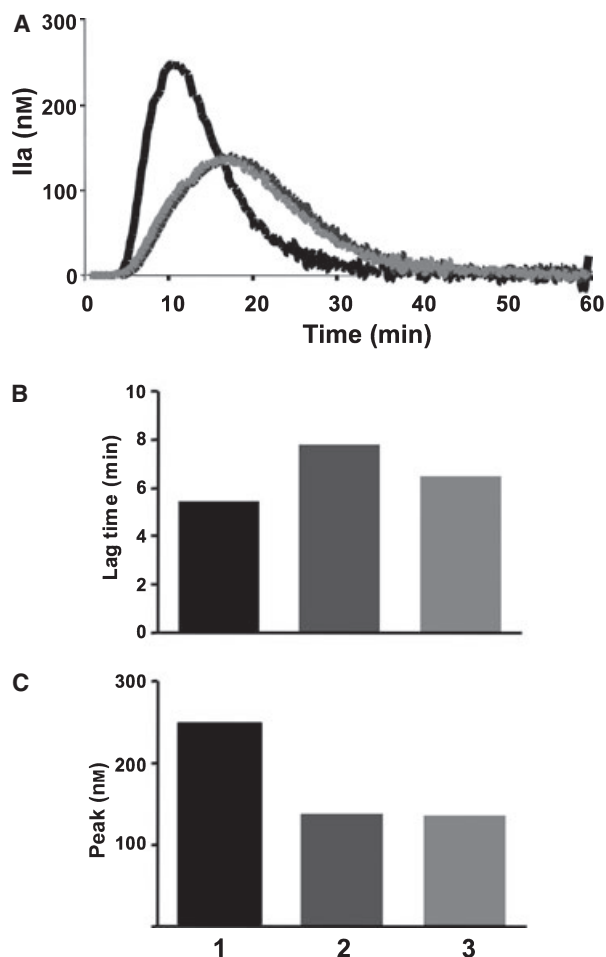


Fig. 5. Effect of m_{scFv} 9O12 on thrombin generation induced by collagen in PRP. (A) PRP was preincubated with vehicle (black curve), 9O12 Fab (dark gray) or m_{scFv} 9O12 (light gray) before addition of collagen. Thrombin generation was initiated by adding tissue factor and $CaCl_2$. The thrombin concentration was determined using a fluorescent substrate and was calculated relative to a calibrator. (B, C) The traces are from one representative experiment. Bar graphs represent mean \pm standard deviation of the lag phase (B) and the peak values ($n = 3$) (C). The bars corresponding to the standard deviation are too small to be visible. 1, collagen; 2, 9O12 Fab + collagen; 3, m_{scFv} 9O12 + collagen.

protein (h_{scFv} 9O12) was produced in the periplasm of recombinant ToppI *E. coli* cells and purified to homogeneity by affinity chromatography using GPVI–Sepharose bead columns. A single band with the size expected (28 kDa) was observed after SDS/PAGE. However, the production yield of h_{scFv} 9O12 was very low. We observed a slightly better level of expression when using BL21DE3 *E. coli* transformed with pET-22- h_{scFv} 9O12 ($60 \mu g \cdot L^{-1}$ of culture), and we selected this expression system to produce h_{scFv} 9O12 for further characterization (Fig. 7A). The purified

h_{scFv} 9O12 conserved high affinity for its target, as demonstrated by SPR analysis against immobilized GPVI ($k_{on} = 5.8 \times 10^4 M^{-1} \cdot s^{-1}$, $k_{off} = 1.86 \times 10^{-4} s^{-1}$, and dissociation constant $K_D = 3.2$ nM) (Fig. 7B). It was also able to bind to freshly prepared human platelets in flow cytometry, and the shift to the right of the fluorescence peak was similar to that of cells labeled with m_{scFv} 9O12 under similar experimental conditions (Fig. 7C). Finally, nearly total inhibition of h_{scFv} 9O12 binding was observed when platelets were premixed with an excess of 9O12 Fab. In addition, h_{scFv} 9O12 binding to platelets inhibited platelet activation induced by convulxin which is a specific GPVI agonist [24]. Indeed, P-selectin exposure was not observed at the surface of platelets preincubated with h_{scFv} 9O12 and then activated by convulxin (Fig. 8A). In addition, we observed that h_{scFv} 9O12 inhibited the aggregation of platelets induced by collagen but not by thrombin or the thrombin receptor agonist peptide (TRAP), which demonstrates that h_{scFv} 9O12 inhibition is GPVI-dependent (Fig. 8B).

Discussion

Platelets play a crucial role in arterial thrombosis and represent a major therapeutic target. All the drugs currently available act on late phases of thrombus formation, and their use is often associated with major drawbacks, such as prolongation of the bleeding time and/or induction of thrombocytopenia. Acting at an earlier stage of the platelet aggregation process could offer several advantages. GPVI and GPIa–IIa are the main platelet receptors, interacting directly with the collagen exposed by the subendothelial matrix as a result of vascular injury, but GPVI is the only one specifically expressed at the surface of platelets. Early GPVI interaction with collagen is a major event leading to platelet activation, the release of secondary agonists, and thrombus formation. Thus, inhibition of GPVI–collagen interaction could have potent antithrombotic effects. This has been demonstrated both *in vitro* and under physiological conditions *in vivo*. Deficiency in GPVI expression does not lead to impaired hemostasis in mice or humans [6,10]. Furthermore, anti-GPVI molecules inhibit thrombus growth without producing any significant side effects [8,10].

In this context, the need for better antithrombotic drugs, and the emergence of numerous antibody-derived molecules approved for the treatment of a wide range of disorders, have stimulated the search for potent antithrombotic antibodies. This is exemplified by the chimeric mouse–human Fab abciximab

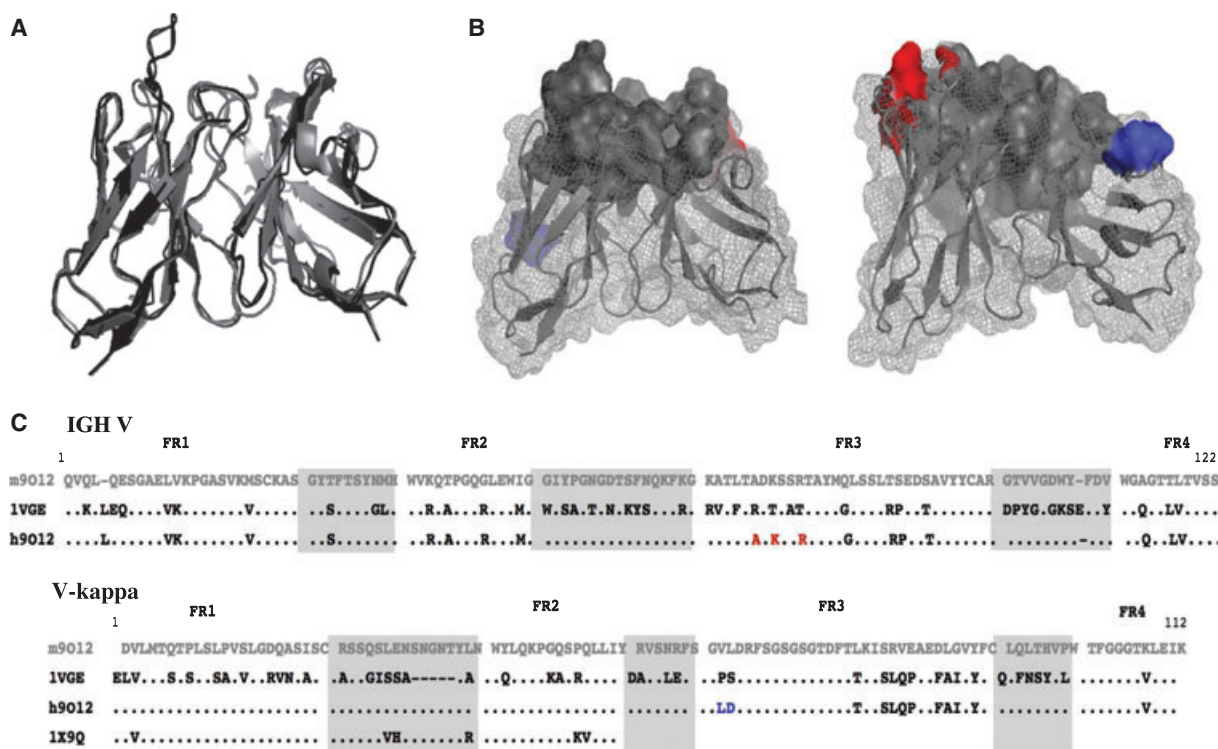


Fig. 6. Humanization of the 9012 antibody variable domains. (A) Superimposed variable domain ribbon diagram of murine 9012 (gray) and human 1VGE (black) antibodies in lateral view. (B) Models of the humanized 9012 variable domains in both lateral views. CDRs are shown in surface representation, and frameworks in ribbon representation. Framework residues having no similarity with their counterparts in human antibody sequences are shown in blue (V-kappa FR3) or in red (IGHV FR3). (C) Sequence analysis of antibody IGHV and kappa-V domains: murine 9012 (m9012); 1VGE; humanized 9012 (h9012); and 1X9Q. (.) indicates residues identical to murine 9012. (-) indicates a gap. Residues of the humanized variable domains having no similarity with murine 9012 are shown in red and blue (residues A71, K73 and R76 for IGHV, and L59 and D60 for kappa-V; numbering according to the Kabat nomenclature). CDRs are highlighted in gray.

Table 1. Identity and similarity scores of the 9012 humanized variable domain frameworks, with human antibody frameworks used as template; x is the number of residues in the humanized FR that are identical to residues from the human FR; y is the total number of residues in the FR.

Domain	Identity (x/y)	Identity (%)	Similarity (%)
IGHV domain			
FR1	23/26	88.46	100
FR2	14/14	100	100
FR3	25/32	78.12	90.62
FR4	11/11	100	100
V-kappa domain			
FR1	22/23	95.65	100
FR2	13/15	86.60	100
FR3	30/32	93.75	93.75
FR4	10/10	100	100

(Reopro[®]), which blocks the platelet GPIIb-IIIa receptor, and is now used for the treatment of patients with acute coronary syndrome undergoing percutaneous coronary surgery [25,26].

Few antibody molecules directed against GPVI have been prepared, because GPVI cDNA has only recently been cloned and expressed as a recombinant soluble protein [5,27]. Some anti-GPVI scFvs have been selected after panning phage libraries expressing non-immune human repertoires [13–15]. However, this approach has not yet been demonstrated to be fully effective. Indeed, although some of the anti-GPVI scFvs isolated do lead to dose-dependent inhibition of the GPVI–collagen interaction *in vitro*, they have a weak affinity for GPVI, making them unsuitable for clinical investigations. Such difficulties may be related to technical problems, including difficulties in constructing large libraries of scFvs, maintaining the repertoire over time, and slowing its inevitable drift [28].

All of the high-affinity antibodies against GPVI isolated so far have been prepared using the more conventional hybridoma technology after immunization of Balb/C mice with 3T3 fibroblasts expressing human GPVI or with the cDNA encoding the human GPVI protein, as is the case for 9012, or after inoculation of

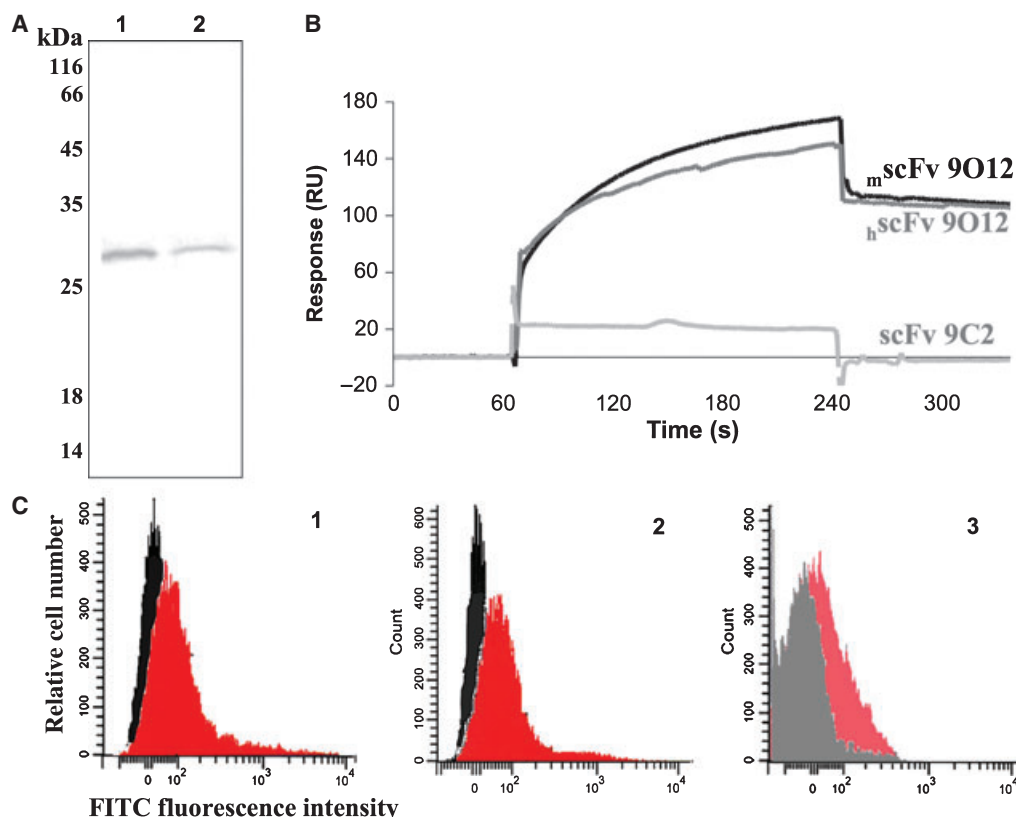


Fig. 7. Characterization of $hscFv$ 9O12. (A) Western blot detection of recombinant scFvs using antibody against c-Myc. 1, $mScFv$ 9O12; 2, $hScFv$ 9O12. (B) SPR analysis. GPVI was immobilized on a CM5 sensor chip, and the binding of purified scFv ($10 \mu\text{g}\cdot\text{mL}^{-1}$) was analyzed. 1, $mScFv$ 9O12; 2, $hScFv$ 9O12; 3, control scFv 9C2. (C) Flow cytometry analysis. Washed human platelets were incubated with antibody fragments (red histogram), and bound antibody was detected using an FITC-coupled antibody against c-Myc. Panels 1 and 2: $mScFv$ 9O12 (1) and $hScFv$ 9O12 (2) are shown in red, and the control scFv 9C2 in black. Panel 3: platelets preincubated with 9O12 Fab (gray histogram) or not (red histogram) were then incubated with $hScFv$ 9O12.

GPVI-knockout mice with transfected Chinese hamster ovary cells expressing human GPVI and FcR γ , as has recently been reported [17,18,20,29]. Some of these antibodies are devoid of blocking activity, such as HY101, 6B12, and 3J24.2 [29–31]. Others have good potential in terms of their biological and pharmacological properties, displaying direct blocking activity against the GPVI–collagen interaction when tested as monovalent Fab fragments. In addition, the *ex vivo* antithrombotic effects of anti-GPVI Fabs obtained by papainolysis of murine IgGs OM4 and 9O12 have been observed in nonhuman primates without the induction of platelet GPVI depletion [18,32]. For all of these reasons, 9O12 is an excellent template to use when designing antithrombotic molecules with potential human clinical applications.

Murine antibodies are highly immunogenic when injected into humans, and thus they have to be chimerized or humanized for therapeutic applications [33]. Chimerization is achieved by transferring variable

domains to human constant antibody domains. The chimeric Fab abciximab, which binds to the platelet fibrinogen receptor GPIIb–IIIa, inhibits thrombus growth, but it still induces adverse immune responses against mouse epitopes in small groups of patients [34]. A humanized antibody, ‘eculizumab’, has recently been approved by the US Food and Drug Administration for the chronic treatment of paroxysmal nocturnal hemoglobinuria. It is nonimmunogenic, safe, and well tolerated [35]. Several possible methods of humanizing antibody variable domains have been suggested [36–38]. None of these methods is simple, and all often result in impaired specificity and/or affinity [39–42].

In view of the functional properties of the murine 9O12 Fab fragment, we designed and evaluated the activity of derived scFvs that can be viewed as possible building blocks for future drug development. First, murine scFv 9O12 was engineered with the intention of determining the 9O12 variable domain sequences and checking their functionality when produced as a

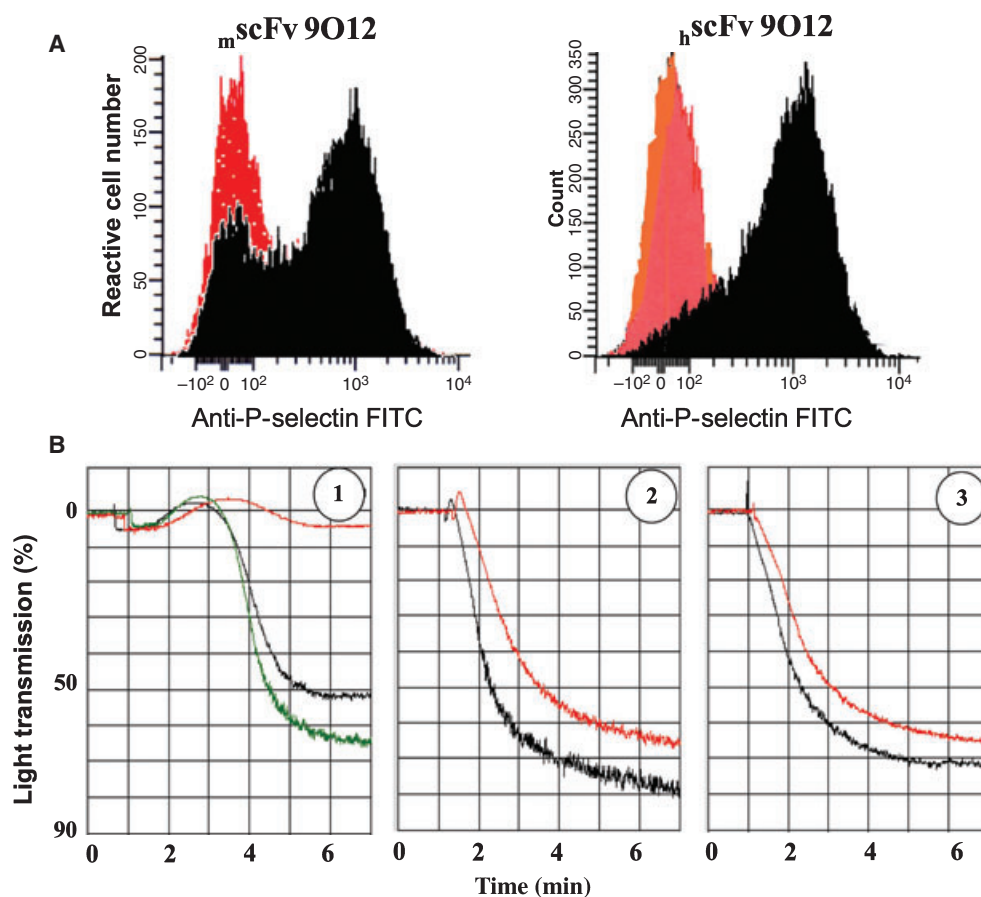


Fig. 8. Effects induced by *h*scFv 9O12 binding on platelet activation and aggregation. (A) P-selectin exposure: washed human platelets were preincubated with NaCl/P_i (black histograms) or the antibody fragments (red histograms) for 30 min, and then activated by convulxin. P-selectin exposure was detected using FITC-conjugated antibody against P-selectin. (B) Effects of *h*scFv 9O12 on platelet aggregation: washed human platelets were incubated alone (dark line), with affinity-purified *h*scFv 9O12 (red line), or with the flow-through fraction collected upon affinity purification of *h*scFv 9O12 (green line). Aggregation was induced with collagen (1), thrombin (2), or TRAP (3).

recombinant molecule in a heterologous expression system. Affinity-purified scFv preserved high functional affinity for GPVI, which allowed it to block collagen-induced platelet aggregation, and inhibit thrombus formation under flow conditions as well as preventing thrombin generation. To reduce the immunogenicity of *m*scFv, we then proceeded to humanize it by a procedure essentially based on CDR grafting combined with refinements based on *in silico* modeling. The final product reported here exhibits 100% similarity with human antibody frameworks, with the exception of VH FR3 (90.62%) and VL FR3 (93.75%), and its framework sequences differ by 25 residues from that of *m*scFv 9O12. The strategy consisted of grafting murine CDRs onto the frameworks of human antibody 1VGE in order to preserve interdomain contacts. This strategy was effective, but required further refinement. Indeed, during this first attempt, the recombinant scFv resulting from the grafting of 9O12 CDRs onto 1VGE

frameworks was not produced efficiently. We postulated unforeseen structural incompatibilities between the original murine CDRs and the human acceptor frameworks that could have led to misfolding of the variable domains. To circumvent these difficulties, some minor refinements were made. First, we observed that 9O12 V-kappa CDR1 is particularly long and has five more residues than 1VGE, suggesting that 1VGE V-kappa FR1 and FR2 are not suitable for the correct folding of CDR1. Back-mutation to 9O12 wild-type V-kappa FR1 and FR2 was therefore required, and this was encouraged by the observation that the sequences of these murine frameworks fit well with another human antibody framework (1X9Q). V-kappa CDR1 of antibody 1X9Q is exactly the same size as that of 9O12 (Fig. 6). We also retained in the final construct a very limited number of residues that could influence the ability of CDR loops to adopt their conformation.

Two critical areas were preserved. The first one was the dipeptide Leu-Asp at position 59–60 in the V-kappa domain. Leu59 (Pro in the human template) was considered to be potentially significant, as it is in the close vicinity of the residues of V-kappa CDR2. Although Leu and Pro are both hydrophobic, Pro has a cyclical side chain and is known to have specific effects on the protein backbone structure [43]. In addition, we noticed that Leu occurs much less often than Pro at this position (2%), and this may be indicative of a specific role [44]. The other unmutated murine residues with no similarities to the human template (1VGE) were located in IGHV FR3 (Ala71, Lys73, and Arg76; Kabat numbering). *In silico* observations and previous analysis have shown that Ala71 has an important role in the conformation of IGHV CDR2 [45]. Finally, only five murine residues in V-kappa and 10 in IGHV were maintained in the human frameworks selected for humanization. Other humanized scFvs reported in the literature have almost always required the insertion of numerous murine residues into the reshaped molecule in order to preserve strong binding activity and specificity [46]. FASTA searches of the final humanized IGHV and V-kappa sequences (with the exclusion of the CDRs) against the UniProt data bank showed that the five best-fitting sequences were all derived from human antibodies, whereas the same search performed for murine 9O12 variable domains led exclusively to murine antibody sequences.

The main parameters usually affected by humanization were well preserved in our final product. Affinity-purified $_{\text{h}}\text{scFv}$ 9O12 was fully functional, with high affinity for GPVI, a major point for biological applications. Fluorescence-activated cell sorting analysis also indicated that $_{\text{h}}\text{scFv}$ 9O12 recognizes the same epitope on human platelets as mouse 9O12 Fab, because its binding was specifically blocked in the presence of a molar excess of 9O12 Fab. However, despite the use of codons optimized for prokaryotic expression in the synthetic cDNA encoding $_{\text{h}}\text{scFv}$ 9O12, the production yield remained low, and other expression systems will have to be tested in the future [47,48]. For this reason, the ability of $_{\text{h}}\text{scFv}$ to inhibit aggregation in flow conditions was not investigated here. However, we clearly demonstrate that binding of $_{\text{h}}\text{scFv}$ 9O12 inhibits GPVI-dependent platelet activation and aggregation.

In conclusion, this study provides the first experimental evidence that murine anti-human GPVI platelets can be humanized without deleterious effects, making $_{\text{h}}\text{scFv}$ 9O12 a powerful building block for the generation and evaluation of new compounds with potentially therapeutic antithrombotic properties.

Experimental procedures

Materials

Hybridoma cell line 9O12 secreting a monoclonal IgG_{1,k} directed against the GPVI of human platelets, and IgG and Fab fragment preparation and purification, have been reported previously [20]. The scFv 9C2 directed against a scorpion toxin, irrelevant to GPVI, was prepared as in [49]. The antibody against flag (9E10) was used either free or conjugated to horseradish peroxidase (Sigma-Aldrich, Saint Quentin Fallavier, France) or to fluorescein isothiocyanate (FITC) (Invitrogen, Cergy Pontoise, France). FITC-coupled goat anti-mouse IgGs were from Sigma-Aldrich.

The recombinant soluble human GPVI protein, consisting of two extracellular domains of the receptor, coupled to the Fc fragment of human IgG₁ was produced and purified as in [20]. GPVI was coupled to cyanogen bromide-activated Sepharose according to the manufacturer's instructions (Amersham-Pharmacia, Les Ulis, France). The gel was stored at 4 °C in NaCl/P_i containing sodium azide (1%).

Blood was collected from healthy volunteers. Washed human platelets were obtained according to a previously described procedure [24].

All chemicals were of standard grade from Sigma-Aldrich or equivalent.

Construction of the single chain antibody genes

mRNA was isolated from freshly subcloned hybridoma 9O12. cDNAs encoding the antibody variable domains (V-kappa and IGHV) were cloned after RT-PCR, essentially as previously reported [21,22]. Murine scFv 9O12 was created by PCR splicing with overlap extensions using oligonucleotides that encode the (G₄S)₃ peptide linker between the C-terminus of IGHV and the N-terminus of V-kappa. First, IGHV and V-kappa genes were modified by PCR amplification with primers VHRev and VHlinkFor or VLlinkRev and VLFor, respectively. VHRev (5'-CAG GTG CAG CTG CAG GAG TCA GG-3') encoded the N-terminal sequence of IGHV containing a *Pst*I site, and VHlinkFor (5'-ACC ACC GGA TCC GCC TCC GCC TGA GGA GAC GGT GAC CGT-3') encoded the C-terminus of IGHV and part of the linker. VLlinkRev (5'-GGA GGC GGA TCC GGT GGT GGC GGA TCT GGA GGT GGC GGA AGC GAT GTT TTG ATG ACC CAA ACT CCA CT-3') and VLFor (5'-GAC CCT CGA GCG TTT GAT CTC CAG CTT GGT-3'), which contains a *Xho*I site, were used to amplify and modify the V-kappa domain. Both genes were assembled by 'splicing by overlap extension' with primers VHRev and VLFor. The gene fragment of the appropriate size was purified, cleaved with *Pst*I and *Xho*I, and cloned into the expression vector pSWI restricted in the same manner before being sequenced. This made it possible to clone the scFv gene in-frame with the

pelB leader sequence at its 5'-end and, downstream, a sequence encoding the c-Myc tag. The constructed vector pSW_{-h}scFv9O12 was cloned into the Toppl *E. coli* strain (Stratagene, La Jolla, USA).

Computational analysis and synthetic gene design

Frameworks and the hypervariable loops (CDRs) of antibody variable domains were identified using the Kabat nomenclature [50]. An *in silico* 3D model of 9O12 Fv was constructed by homology modeling based on V-kappa and IGHV domains with maximum sequence identity and a known tertiary structure. First, the protein structure sequence Protein Data Bank was searched for antibody sequence similarities with each individual 9O12 variable domain, using the FASTA 3 program at the European Bioinformatics Institute (EMBL-EBI, Cambridge, UK). Then, MODELER 3.0 software (Accelrys, San Diego, CA, USA) was used to generate up to 20 models for each variable domain, the best one being selected on the basis of the rmsd value.

To design a humanized scFv (hscFv), the 9O12 variable domain sequences were independently subjected to a FASTA search against the Protein Data Bank, and the closest human antibody variable domains were selected. The same search was also performed after excluding the CDR regions. The scaffolds of variable domains belonging to the same antibody molecule were chosen in order to minimize the risk of lowering the stability of the interaction between variable domains in the recombinant scFvs while attempting to preserve the scaffold required for the integrity of the antigen-binding site. In the first step, the human antibody 1VGE variable domains were selected as templates, and the murine 9O12 CDRs were grafted onto them *in silico*. The framework sequences were inspected to see whether any buried residues had been conserved. The packing of the grafted loops was also evaluated by visual inspection, and FR refinements were performed by *in silico* substitution.

The changes in the amino acids required for the humanization were obtained by *de novo* DNA synthesis. Optimization of the DNA design was performed using the codon usage table for expression in *E. coli* cells [51]. Restriction sites were also inserted at the extremities of the CDRs to make it possible to carry out the cDNA sequence adjustments that would be required to optimize the structural or functional characteristics of the recombinant protein. The synthetic gene encoding hscFv 9O12 was cloned into the expression vector pSW1 restricted with *Pst*I and *Xho*I, leading to a vector designated pSW_{-h}scFv 9O12, which allows periplasmic expression of hscFv 9O12 fused to the c-Myc tag. The gene encoding hscFv 9O12 fused to the c-Myc tag was also cloned into the pET-22b(+) vector (Merck Chemicals Ltd., Nottingham, UK), which carries a T7

promoter. To do this, the sequence encoding hscFv 9O12 fused to the c-Myc tag was first reamplified from pSW_{-h}scFv 9O12 by PCR using primers VHPetRev (5'-TG GCC ATG GCC CAG GTG CAG CTG CAG G-3') and 9O12pEtFor (5'-TG GTG CGG CCG CTT ATT AAT TCA GAT CCT CTT CTG A-3'). The amplified cDNA was then digested with *Nco*I and *Not*I, leading to a 820 bp sequence that was cloned in-frame with the pelB leader sequence into pET-22b(+) restricted in the same manner. The constructed vector, designated pET-22_{-h}scFv 9O12, was cloned into the BL21DE3 *E. coli* strain (Merck Chemicals Ltd.).

Production and purification of recombinant antibody fragments

For expression of the recombinant scFvs, bacteria containing the desired plasmids were grown in 500 mL of 2× TY medium (Difco, Le Pont de Claix, France) containing ampicillin (100 µg·mL⁻¹) at 37 °C under rotative agitation (125 r.p.m.), until $A_{600\text{ nm}}$ reached 0.6 (BL21DE3 *E. coli*) or 1.5 (Toppl *E. coli*). Then, 0.8 mM isopropyl-thio-β-D-galactoside was added to the medium, and incubation was continued for 16 h at 16 °C under rotative agitation (75 r.p.m.) to induce scFv production. Bacteria were then collected by centrifugation (3600 g, 20 min, 4 °C). Periplasmic extracts containing scFv were prepared by resuspending the pellet in 10 mL of ice-cold TES buffer (0.2 M Tris/HCl, pH 8.0, containing 0.5 mM EDTA and 0.5 M sucrose), and incubating for 30 min. Cells were subjected to osmotic shock by adding TES buffer diluted 1 : 4 for 30 min on ice, and then centrifuging at 15 000 g for 30 min at 4 °C to remove insoluble material. Deoxyribonuclease A (50 U) and aprotinin (2 µg·mL⁻¹) were added to the supernatant before extensive dialysis against NaCl/P_i at 4 °C.

To purify scFv, the periplasmic extract (30 mL) was incubated with 500 µL of GPVI coupled to Sepharose beads for 12 h at 4 °C and for 4 h at room temperature. The mixture was loaded onto a microcolumn. After washing with NaCl/P_i at pH 7.4, bound proteins were eluted with 0.1 M glycine-HCl (pH 3.0) in 0.4 mL fractions, and immediately neutralized with 5 µL of 3 M Tris on ice. Fractions with $A_{280\text{ nm}}$ higher than 0.2 were pooled and extensively dialyzed against NaCl/P_i.

The purity was checked by SDS/PAGE using a 15% gel followed by staining with Coomassie brilliant blue, or by western blotting and immunostaining with horseradish peroxidase-coupled antibody against c-Myc, essentially as in [22]. The integrity of the purified recombinant protein was also investigated by MALDI-TOF MS on a 4700 Proteomics Analyzer MALDI-time of flight (TOF)/TOF apparatus (Applied Biosystems, Foster City, CA, USA).

Finally, the affinity-purified scFv (200 µL, 100 µg·mL⁻¹) was analyzed by gel filtration using a Superdex 75 column

(Amersham Bioscience, Les Ulis, France) calibrated using standards from Boehringer Mannheim (Meylan, France). Proteins were eluted with NaCl/P_i at a flow rate of $0.5 \text{ mL}\cdot\text{min}^{-1}$, and detected with a UV recorder at 280 nm.

The concentration of the purified scFvs was evaluated after measuring their absorbance at 280 nm, and using the Swiss Institute of Bioinformatics software (PROTPARAM tool) to determine the theoretical molecular mass of the recombinant scFvs and their extinction coefficient [52]. Affinity-purified $_{\text{h}}\text{scFv}$ 9O12 was aliquoted and stored at -20°C in NaCl/P_i containing 0.1% BSA until further use.

Immunochemical characterization of the scFv fragments

ELISA

Microtitration plates were coated with GPVI in NaCl/P_i ($10 \mu\text{g}\cdot\text{mL}^{-1}$, $100 \mu\text{L}$ per well) overnight at 4°C . Nonspecific binding sites were saturated with $100 \mu\text{L}$ of 1% BSA in NaCl/P_i for 90 min. The plates were then incubated with increasing concentrations of the scFv preparation ($0\text{--}20 \mu\text{g}\cdot\text{mL}^{-1}$; $100 \mu\text{L}$) for 90 min. They were incubated for an additional 90 min with peroxidase-coupled antibody against c-Myc ($100 \mu\text{L}$, $1:750$ in NaCl/P_i). All incubations were carried out at room temperature. Finally, $100 \mu\text{L}$ of the substrate solution (orthophenylene diamine; Sigma-Aldrich) was added to each well for 5 min, and the absorbance was read at 492 nm. Two controls were performed: the first one used the irrelevant scFv 9C2 instead of scFv 9O12, and for the second, coating with GPVI was omitted. Five washes with NaCl/P_i containing 0.05% Tween and $0.1 \text{ mg}\cdot\text{mL}^{-1}$ BSA were performed between each of the intermediate steps. In competitive assays, scFv 9O12 ($100 \mu\text{g}\cdot\text{mL}^{-1}$) was mixed with increasing concentrations of 9O12 ($0\text{--}100 \mu\text{g}\cdot\text{mL}^{-1}$), before being delivered into GPVI-coated microtitration wells. Bound scFv was detected as described above.

SPR

The BIAcore 2000 instrument and all the reagents for analysis were obtained from BIAcore. GPVI was immobilized (approximately 600 RU) on a carboxymethyl dextran CM5 sensor chip activated with a 1:1 mix of *N*-hydroxysuccinimide (50 mM) and *N*-ethyl-*N'*-(dimethylaminopropyl)-carbo-di-imide (200 mM) by a 7 min pulse. Affinity-purified antibody fragments were then passed over the immobilized GPVI in HBS-EP buffer [0.01 M HEPES (pH 7.4), 0.15 M NaCl, 0.005% polysorbate 20 (v/v)] at a flow rate of $20 \mu\text{L}\cdot\text{min}^{-1}$ at 25°C . Glycine-HCl (10 mM, pH 2.5) was injected for 30 s at $20 \mu\text{L}\cdot\text{min}^{-1}$ to regenerate the sensor chip between successive samples. Kinetic constants (k_{on} , k_{off}) were deduced from the analysis of association and dissociation rates at four different antibody fragment

concentrations, ranging from 5 to $40 \mu\text{g}\cdot\text{mL}^{-1}$. The dissociation constant K_{D} was calculated from $K_{\text{D}} = k_{\text{off}}/k_{\text{on}}$. Sensorgrams were analyzed using BIAEVALUATION version 3.1 software. All experiments were carried out in quadruplicate at the Institute Jacques Monod platform (Paris, France).

Flow cytometry

scFv binding

Washed human platelets ($2 \times 10^7 \text{ mL}^{-1}$) from several healthy volunteers were incubated for 30 min at room temperature with $10\text{--}40 \mu\text{g}\cdot\text{mL}^{-1}$ purified scFv, and then incubated again for 30 min at room temperature with $5 \mu\text{L}$ of FITC-coupled anti-c-Myc IgG (dilution 1:60). Cell fluorescence was measured using a flow cytometer (Epics XL, Beckman Coulter, Villepinte, France). Background was determined by using the irrelevant scFv 9C2 instead of the scFv 9O12 variants. All incubations were carried out in the dark. When 9O12 Fab ($40 \mu\text{g}\cdot\text{mL}^{-1}$) binding to platelets was investigated, FITC-conjugated goat anti-(mouse IgG) (Sigma-Aldrich) (1:100) was used instead of the FITC-coupled anti-c-Myc IgG.

scFv binding inhibition

Cells were incubated with blocking Fab 9O12 ($10 \mu\text{g}\cdot\text{mL}^{-1}$) for 10 min. They were then mixed with purified $_{\text{h}}\text{scFv}$ 9O12 ($40 \mu\text{g}\cdot\text{mL}^{-1}$), and incubated for 30 min. Finally, $5 \mu\text{L}$ of FITC-coupled anti-c-Myc IgG (diluted 1:60) was added to the cells for a further 30 min before analysis of the cell suspension by flow cytometry.

Inhibition of platelet activation

Platelets were incubated for 30 min. with scFv ($10\text{--}40 \mu\text{g}\cdot\text{mL}^{-1}$) or NaCl/P_i . Then, platelets were activated with convulxin (0.3 nM) for 15 min at 20°C . Five microliters of an anti-P-selectin IgG conjugated to FITC (Beckman Coulter, Villepinte, France) was added to the cells for 30 min before analysis of the cell suspension by flow cytometry. All experiments were carried out at least in triplicate.

Ability of the antibody fragments to block GPVI binding to collagen

Wells of a microtitration plate (Immulon 2; Dynex, VWF, France) were coated overnight with $100 \mu\text{L}$ of collagen type I (equine tendon; Horm, Nycomed, Munich) ($20 \mu\text{g}\cdot\text{mL}^{-1}$) and blocked with BSA (0.2% in NaCl/P_i) for 2 h. Then, $100 \mu\text{L}$ of GPVI (10 , 20 or $40 \mu\text{g}\cdot\text{mL}^{-1}$) that had been preincubated for 30 min with increasing amounts of antibody fragments ($0\text{--}20 \mu\text{g}\cdot\text{mL}^{-1}$) was added to each well. After incubation for 2 h, the bound GPVI was detected

using a peroxidase-coupled anti-human Fc (Jackson Immuno-Research Labs Inc., West Grove, PA, USA) and orthophenylene dimine. All incubations were performed at room temperature, and five washes with 300 μL of NaCl/P_i containing 0.1% Tween-20 and 1% BSA were carried out between each step. All assays were conducted in triplicate. The percentage of residual GPVI binding to collagen was determined using mean values.

Platelet aggregation assays

Platelet aggregation

Washed human platelets ($3 \times 10^8 \text{ mL}^{-1}$) were preincubated for 5 min at 37 °C with antibody fragments in NaCl/P_i ($25 \mu\text{g}\cdot\text{mL}^{-1}$), without stirring. Platelet aggregation was then initiated by adding type I collagen to a final concentration of $1 \mu\text{g}\cdot\text{mL}^{-1}$, or thrombin (1 nM) or the thrombin receptor agonist peptide TRAP (10 μM) [20]. Platelet aggregation induced changes in light transmission that were continuously recorded (Chronolog Aggregometer Chrono Log Corp., Harveston, PA, USA).

Platelet aggregation under flow conditions

Platelet adhesion to collagen under flow conditions was measured essentially as described previously [20]. Glass coverslips were coated with fibrillar type I collagen ($50 \mu\text{g}\cdot\text{mL}^{-1}$). Blood from healthy volunteers was collected on 40 μM PPACK, and labeled with DIOC-6 (1 μM). Blood aliquots were incubated for 15 min at room temperature with buffer or purified antibody fragment (9O12 Fab, mScFv 9O12, scFv 9C2) at a final concentration of $50 \mu\text{g}\cdot\text{mL}^{-1}$. The mixture was then perfused over the collagen-coated coverslips inserted in a flow chamber at 1500 s^{-1} for 5 min. Transmission and fluorescent images were recorded in real time using a fluorescence microscope. Fluorescent images were obtained from at least 10 different collagen-containing microscopic fields, which were arbitrarily chosen at the end of perfusion. The area coverage of fluorescent images was analyzed off-line using HISTOLAB software (Microvision, Evry, France). Assays were performed using blood from two healthy volunteers and two distinct preparations of affinity-purified scFv.

Thrombin generation

Thrombin generation was continuously measured in platelet-rich plasma (PRP) using the thrombogram method as previously described [53]. Briefly, citrated PRP ($1.5 \times 10^8 \text{ platelets mL}^{-1}$) was incubated with the antibody fragments ($50 \mu\text{g}\cdot\text{mL}^{-1}$) for 10 min at 37 °C before addition of the collagen ($5 \mu\text{g}\cdot\text{mL}^{-1}$). Ten minutes later, thrombin generation was initiated by transferring the samples into the wells of a microtitration plate containing tissue factor

(0.5 μM). After 5 min at 37 °C, the reaction was initiated by addition of buffer containing CaCl_2 (16.6 mM) and the fluorescent thrombin substrate Z-GGR-AMC (Stago, Asnières, France). Fluorescence accumulation of the cleaved substrate was continuously measured at excitation and emission wavelengths of 390 and 460 nm, respectively. First derivative curves of fluorescence accumulation were converted into thrombin concentration curves using a thrombin calibrator [54]. The peak height is an indicator of the maximum rate of thrombin formation, and is sensitive to platelet activation.

Acknowledgements

We are indebted to J. M. Camadro for stimulating discussions. We also acknowledge the invaluable technical help provided by S. Loyau. J. Muzard was a research fellow of Stago (Asnières, France) and the Fondation pour la Recherche Médicale (FRM). This work was supported by grant no. 2007001960 from the Fondation de France and grant no. 07-EMPB-002-01 from the Agence Nationale de la Recherche (ANR).

References

- Bhatt DL & Topol EJ (2003) Scientific and therapeutic advances in antiplatelet therapy. *Nat Rev Drug Discov* **2**, 15–28.
- Jackson SP & Schoenwaelder SM. (2003) Antiplatelet therapy: in search of the ‘magic bullet’. *Nat Rev Drug Discov* **2**, 775–789.
- Lindemann S, Kramer B, Daub K, Stellos K & Gawaz M (2007) Molecular pathways used by platelets to initiate and accelerate atherogenesis. *Curr Opin Lipidol* **18**, 566–573.
- Konishi H, Katoh Y, Takaya N, Kashiwakura Y, Itoh S, Ra C & Daida H (2002) Platelets activated by collagen through immunoreceptor tyrosine-based activation motif play pivotal role in initiation and generation of neointimal hyperplasia after vascular injury. *Circulation* **105**, 912–916.
- Jandrot-Perrus M, Busfield S, Lagrue AH, Xiong X, Debili N, Chickering T, Le Couedic JP, Goodearl A, Dussault B, Fraser C *et al.* (2000) Cloning, characterization, and functional studies of human and mouse glycoprotein VI: a platelet-specific collagen receptor from the immunoglobulin superfamily. *Blood* **96**, 1798–1807.
- Moroi M, Jung SM, Okuma M & Shinmyozu K. (1989) A patient with platelets deficient in glycoprotein VI that lack both collagen-induced aggregation and adhesion. *J Clin Invest* **84**, 1440–1445.
- Boylan B, Chen H, Rathore V, Paddock C, Salacz M, Friedman KD, Curtis BR, Stapleton M, Newman DK, Kahn ML *et al.* (2004) Anti-GPVI-associated ITP:

- an acquired platelet disorder caused by autoantibody-mediated clearance of the GPVI/Fc γ chain complex from the human platelet surface. *Blood* **104**, 1350–1355.
- 8 Massberg S, Konrad I, Bultmann A, Schulz C, Munch G, Peluso M, Lorenz M, Schneider S, Besta F, Muller I *et al.* (2004) Soluble glycoprotein VI dimer inhibits platelet adhesion and aggregation to the injured vessel wall in vivo. *FASEB J* **18**, 397–399.
 - 9 Gruner S, Prostedna M, Koch M, Miura Y, Schulte V, Jung SM, Moroi M & Nieswandt B (2005) Relative anti-thrombotic effect of soluble GPVI dimer compared with anti-GPVI antibodies in mice. *Blood* **105**, 1492–1499.
 - 10 Nieswandt B, Schulte V, Bergmeier W, Mokhtari-Nejad R, Rackebrandt K, Cazenave JP, Ohlmann P, Gachet C & Zirngibl H (2001) Long-term antithrombotic protection by in vivo depletion of platelet glycoprotein VI in mice. *J Exp Med* **193**, 459–469.
 - 11 Schulte V, Rabie T, Prostedna M, Aktas B, Gruner S & Nieswandt B (2003) Targeting of the collagen-binding site on glycoprotein VI is not essential for in vivo depletion of the receptor. *Blood* **10**, 3948–3952.
 - 12 Massberg S, Gawaz M, Gruner S, Schulte V, Konrad I, Zohlnhofer D, Heinzmann U & Nieswandt B (2003) A crucial role of glycoprotein VI for platelet recruitment to the injured arterial wall in vivo. *J Exp Med* **197**, 41–49.
 - 13 Qian MD, Villeval JL, Xiong X, Jandrot-Perrus M, Nagashima K, Tonra J, McDonald K, Goodearl A & Gill D (2002) Anti GPVI human antibodies neutralizing collagen-induced platelet aggregation isolated from a combinatorial phage display library. *Hum Antibodies* **11**, 97–105.
 - 14 Smethurst PA, Joutsu-Korhonen L, O'Connor MN, Wilson E, Jennings NS, Garner SF, Zhang Y, Knight CG, Dafforn TR, Buckle A *et al.* (2004) Identification of the primary collagen-binding surface on human glycoprotein VI by site-directed mutagenesis and by a blocking phage antibody. *Blood* **103**, 903–911.
 - 15 Siljander PR, Munnix IC, Smethurst PA, Deckmyn H, Lindhout T, Ouwehand WH, Farndale RW & Heemskerk JW (2004) Platelet receptor interplay regulates collagen-induced thrombus formation in flowing human blood. *Blood* **103**, 1333–1334.
 - 16 Matsumoto Y, Takizawa H, Nakama K, Gong X, Yamada Y, Tandon NN & Kambayashi J (2006) *Ex vivo* evaluation of anti-GPVI antibody in cynomolgus monkeys: dissociation between anti-platelet aggregatory effect and bleeding time. *Thromb Haemost* **96**, 1671–1675.
 - 17 Matsumoto Y, Takizawa H, Gong X, Le S, Lockyer S, Okuyama K, Tanaka M, Yoshitake M, Tandon NN & Kambayashi J (2007) Highly potent anti-human GPVI monoclonal antibodies derived from GPVI knockout mouse immunization. *Thromb Res* **119**, 319–329.
 - 18 Li H, Lockyer S, Concepcion A, Gong X, Takizawa H, Guertin M, Matsumoto Y, Kambayashi J, Tandon NN & Liu Y (2007) The Fab fragment of a novel anti-GPVI monoclonal antibody, OM4, reduces in vivo thrombosis without bleeding risk in rats. *Arterioscler Thromb Vasc Biol* **27**, 1199–1205.
 - 19 Takayama H, Hosaka Y, Nakayama K, Shirakawa K, Naitoh K, Matsusue T, Shinozaki M, Honda M, Yata-gai Y, Kawahara T *et al.* (2008) A novel antiplatelet antibody therapy that induces cAMP-dependent endo-cytosis of the GPVI/Fc receptor gamma-chain complex. *J Clin Invest* **118**, 1785–1795.
 - 20 Lecut C, Feeney LA, Kingsbury G, Hopkins J, Lanza F, Gachet C, Villeval JL & Jandrot-Perrus M (2003) Human platelet glycoprotein VI function is antagonized by monoclonal antibody-derived Fab fragments. *J Thromb Haemost.* **1**, 2653–2662.
 - 21 Juste M, Muzard J & Billiald P (2006) Cloning of the antibody kappa light chain V-gene from murine hybridomas by bypassing the aberrant MOPC21-derived transcript. *Anal Biochem* **349**, 159–161.
 - 22 Devaux C, Moreau E, Goyffon M, Rochat H & Billiald P (2001) Construction and functional evaluation of a single-chain antibody fragment that neutralizes toxin *AahI* from the venom of the scorpion *Androctonus australis hector*. *Eur J Biochem* **268**, 694–702.
 - 23 Lecut C, Schoolmeester A, Kuijpers MJ, Broers JL, van Zandvoort MA, Vanhoorelbeke K, Deckmyn H, Jandrot-Perrus M & Heemskerk JW (2004) Principal role of glycoprotein I in alpha2beta1 and alphaIIb-beta3 activation during collagen-induced thrombus formation. *Arterioscler Thromb Vasc Biol* **24**, 1727–1733.
 - 24 Jandrot-Perrus M, Lagrue AH, Okuma M & Bon C. (1997) Adhesion and activation of human platelets induced by convulxin involve glycoprotein VI and integrin alpha2beta1. *J Biol Chem* **272**, 27035–27041.
 - 25 Kastrati A, Mehilli J, Neumann FJ, Dotzer F, ten Berg J, Bollwein H, Graf I, Ibrahim M, Pache J, Seyfarth M *et al.* (2006) Abciximab in patients with acute coronary syndromes undergoing percutaneous coronary intervention after clopidogrel pretreatment: the ISAR-REACT 2 randomized trial. *JAMA* **295**, 1531–1538.
 - 26 De Luca G, Suryapranata H, Stone GW, Antoniucci D, Tcheng JE, Neumann FJ, Van de Werf F, Antman EM & Topol EJ (2005) Abciximab as adjunctive therapy to reperfusion in acute ST-segment elevation myocardial infarction: a meta-analysis of randomized trials. *JAMA* **293**, 1759–1765.
 - 27 Clemetson JM, Polgar J, Magnenat E, Wells TN & Clemetson KJ (1999) The platelet collagen receptor glycoprotein VI is a member of the immunoglobulin superfamily closely related to FcalphaR and the natural killer receptors. *J Biol Chem* **274**, 29019–29024.

- 28 Laffly E & Sodoyer R (2005) Monoclonal and recombinant antibodies, 30 years after... *Hum Antibodies* **14**, 33–55.
- 29 Chen H, Locke D, Liu Y, Liu C & Kahn ML (2002) The platelet receptor GPVI mediates both adhesion and signaling responses to collagen in a receptor density-dependent fashion. *J Biol Chem* **277**, 3011–3019.
- 30 Gardiner EE, Arthur JF, Kahn ML, Berndt MC & Andrews RK (2004) Regulation of platelet membrane levels of glycoprotein VI by a platelet-derived metalloproteinase. *Blood* **104**, 3611–3617.
- 31 Lagrue-Lak-Hal AH, Debili N, Kingbury G, Lecut C, Le Couedic JP, Villeval JL, Jandrot-Perrus M & Vainchenker W (2001) Expression and function of the collagen receptor GPVI during megakaryocyte maturation. *J Biol Chem* **276**, 15316–15325.
- 32 Ohlmann P, Hechler B, Ravanat C, Loyau S, Herrenscheidt N, Wanert F, Jandrot-Perrus M & Gachet C (2008) *Ex vivo* inhibition of thrombus formation by an anti-glycoprotein VI Fab fragment in non-human primates without modification of glycoprotein VI expression. *J Thromb Haemost.* **6**, 1003–1011.
- 33 Hwang WY & Foote J (2005) Immunogenicity of engineered antibodies. *Methods* **36**, 3–10.
- 34 Curtis BR, Swyers J, Divgi A, McFarland JG & Aster RH (2002) Thrombocytopenia after second exposure to abciximab is caused by antibodies that recognize abciximab-coated platelets. *Blood* **99**, 2054–2059.
- 35 Parker C (2009) Eculizumab for paroxysmal nocturnal haemoglobinuria. *Lancet* **373**, 759–767.
- 36 Tsurushita N, Hinton PR & Kumar S (2005) Design of humanized antibodies: from anti-Tac to Zenapax. *Methods* **36**, 69–83.
- 37 Fontayne A, Vanhoorelbeke K, Pareyn I, Van Rompaey I, Meiring M, Lamprecht S, Roodt J, Desmet J & Deckmyn H (2006) Rational humanization of the powerful antithrombotic anti-GPIIb/alpha antibody: 6B4. *Thromb Haemost* **96**, 671–684.
- 38 Lazar GA, Desjarlais JR, Jacinto J, Karki S & Hammond PW (2007) A molecular immunology approach to antibody humanization and functional optimization. *Mol Immunol* **44**, 1986–1998.
- 39 Jones PT, Dear PH, Foote J, Neuberger MS & Winter G (1986) Replacing the complementarity-determining regions in a human antibody with those from a mouse. *Nature* **321**, 522–525.
- 40 Verhoeyen M, Milstein C & Winter G (1988) Reshaping human antibodies: grafting an antilysozyme activity. *Science* **239**, 1534–1536.
- 41 Caldas C, Coelho V, Kalil J, Moro AM, Maranhão AQ & Brígido MM (2003) Humanization of the anti-CD18 antibody 6.7: an unexpected effect of a framework residue in binding to antigen. *Mol Immunol* **39**, 941–952.
- 42 Gonzales NR, Padlan E, De Pascalis R, Schuck P, Schlom J & Kashmiri SV (2004) SDR grafting of a murine antibody using multiple human germline templates to minimize its immunogenicity. *Mol Immunol* **41**, 863–872.
- 43 MacArthur MW & Thornton JM (1999) Protein side-chain conformation: a systematic variation of chi 1 mean values with resolution – a consequence of multiple rotameric states? *Acta Crystallogr D Biol Crystallogr* **55**, 994–1004.
- 44 Honegger A & Pluckthun A (2001) The influence of the buried glutamine or glutamate residue in position 6 on the structure of immunoglobulin variable domains. *J Mol Biol* **309**, 687–699.
- 45 Tramontano A, Chothia C & Lesk AM (1990) Framework residue 71 is a major determinant of the position and conformation of the second hypervariable region in the VH domains of immunoglobulins. *J Mol Biol* **215**, 175–182.
- 46 Woodle ES, Thistlethwaite JR, Jolliffe LK, Zivin RA, Collins A, Adair JR, Bodmer M, Athwal D, Alegre ML & Bluestone JA (1992) Humanized OKT3 antibodies: successful transfer of immune modulating properties and idiotype expression. *J Immunol* **148**, 2756–2763.
- 47 Humphreys DP & Glover DJ (2001) Therapeutic antibody production technologies: molecules, applications, expression and purification. *Curr Opin Drug Discov Devel* **4**, 172–185.
- 48 Carson KL (2005) Flexibility – the guiding principle for antibody manufacturing. *Nat Biotechnol* **23**, 1054–1058.
- 49 Aubrey N, Devaux C, Sizaret PY, Rochat H, Goyffon M & Billiald P (2003) Design and evaluation of a diabody to improve protection against a potent scorpion neurotoxin. *Cell Mol Life Sci* **60**, 617–628.
- 50 Wu TT & Kabbat EA (1970) An analysis of the sequences of the variable regions of Bence Jones proteins and myeloma light chains and their implications for antibody complementarity. *J Exp Med* **132**, 211–250.
- 51 Sharp PM & Li WH (1986) Codon usage in regulatory genes in *Escherichia coli* does not reflect selection for ‘rare’ codons. *Nucleic Acids Res* **14**, 7737–7749.
- 52 Appel RD, Bairoch A & Hochstrasser DF (1994) A new generation of information retrieval tools for biologists: the example of the ExpASY WWW server. *Trends Biochem Sci* **19**, 258–260.
- 53 Lecut C, Feijge MA, Cosemans JM, Jandrot-Perrus M & Heemskerk JW (2005) Fibrillar type I collagens enhance platelet-dependent thrombin generation via glycoprotein VI with direct support of alpha2beta1 but not alphaIIb beta3 integrin. *Thromb Haemost* **94**, 107–114.
- 54 Hemker HC, Giesen PL, Ramjee M, Wagenvoort R & Béguin S (2000) The thrombogram: monitoring thrombin generation in platelet-rich plasma. *Thromb Haemost* **83**, 589–591.